Mapping the sites of interaction between SecY and SecE by cysteine scanning mutagenesis

Veenendaal, A.K.J.; van der Does, C.; Driessen, A.J.M.

Published in:
The Journal of Biological Chemistry

DOI:
10.1074/jbc.M103912200

Publication date:
2001

THE JOURNAL OF BIOLOGICAL CHEMISTRY
Vol. 276, No. 35, Issue of August 31, pp. 32559–32566, 2001
Printed in U.S.A.

Mapping the Sites of Interaction between SecY and SecE by Cysteine Scanning Mutagenesis*

Received for publication, May 1, 2001, and in revised form, June 29, 2001
Published, JBC Papers in Press, July 9, 2001, DOI 10.1074/jbc.M103912200

Andreas K. J. Veenendaal, Chris van der Does, and Arnold J. M. Driessen‡

From the Department of Microbiology, Groningen Biomolecular Sciences and Biotechnology institute, University of Groningen, Kerklaan 30, 9751 NN Haren, The Netherlands

In *Escherichia coli,* the SecYEG complex mediates the translocation and membrane integration of proteins. Both genetic and biochemical data indicate interactions of several transmembrane segments (TMSs) of SecY with SecE. By means of cysteine scanning mutagenesis, we have identified intermolecular sites of contact between TMS7 of SecY and TMS3 of SecE. The cross-linking of SecY to SecE demonstrates that these subunits are present in a one-to-one stoichiometry within the SecYEG complex. Sites in TMS3 of SecE involved in SecE dimerization are confined to a specific α-helical interface and occur in an oligomeric SecYEG complex. Although cross-linking reversibly inactivates translocation, the contact between TMS7 of SecY and TMS3 of SecE remains unaltered upon insertion of the preprotein into the translocation channel. These data support a model for an oligomeric translocation channel in which pairs of SecYEG complexes contact each other via SecE.

In bacteria, protein translocation and membrane protein insertion is mediated by the translocase. Translocase consists of the SecYEG membrane protein complex, and the peripherally membrane-associated SecA dimer (for review, see Ref. 1). SecA is an ATP-dependent motor protein that drives the stepwise translocation of the precursor protein (preprotein) across the membrane by cycles of ATP binding and hydrolysis (2–4). SecY, SecE, and SecG are integral membrane proteins that together form a heterotrimeric complex (5, 6) that constitutes a high affinity binding site for SecA (7). Recent electron microscopic and biochemical studies indicate that the protein conducting channel is composed of a SecYEG tetramer that is assembled by SecA from mono- and dimeric SecYEG subcomplexes (8).

The SecYEG complex is a member of a highly conserved protein translocation pathway (9). It is homologous to the eukaryotic Sec61p complex, which consists of three subunits, α, β, and γ, that together form the "translocon" of the endoplasmic reticulum membrane (10). SecY and SecE are essential subunits of the translocase. SecY comprises 10 transmembrane segments (TMSs)[1] (Fig. 1), whereas SecE is a small membrane protein that in most bacteria contains only a single TMS. In *Escherichia coli,* SecE contains three TMSs, but only the conserved C-terminal portion including the third TMS is required for activity (11) (Fig. 1). SecY and SecE form a stable complex in the membrane that does not dissociate *in vivo* (12). In the absence of SecE, SecY is degraded by FtsH (13). Mutations located in the cytoplasmic loop 4 (C4) of SecY (14) and C2 and TMS3 of SecE (15) destabilize the SecY-SecE interaction. Many of the so-called *prl* mutations (*p*rotein *l*ocalization) that suppress defects in the signal sequence are present in the *secY* and *secE* genes. Specific combinations of these mutations in SecY (*prlA*) and SecE (*prlG*) result in synthetic lethality, and it has been suggested that this signifies sites of interaction between SecY and SecE (16, 17). According to this hypothesis, the periplasmic loop 1 (P1) of SecY and P2 of SecE are interacting regions, whereas TMS3 of SecE interacts with TMS7 and TMS10 of SecY. Recent studies employing cysteine mutagenesis indeed demonstrated that P1 of SecY and P2 of SecE (18), and TMS2 of SecY and TMS3 of SecE (19), are in close proximity. Most of the conserved residues and *prlA* mutations are clustered in TMSs 2, 7, and 10 of SecY, and together with TMS3 of SecE, they form the conserved core of the SecYE complex. Strikingly, the regions suggested to interact overlap with the regions that have been implicated in the binding of the signal sequence of the preprotein. TMS2 and TMS7 of Sec61α, the yeast homologue of SecY can be cross-linked to the signal sequence of a preprotein (20). Cysteine scanning mutagenesis also showed an interaction between two neighboring SecE molecules that is modulated by the SecA and ATP-dependent initiation of preprotein translocation (19). This observation lends further support for an oligomeric nature of the integral membrane domain of the translocase.

A central question is how the SecYEG complex forms the protein-conducting channel. Therefore, detailed information is required about the molecular architecture of the SecYEG complex. For this purpose, we have initiated a cysteine scanning mutagenesis approach to probe sites of interaction between SecY and SecE (19). The method can also be used to detect dynamic changes in subunit interactions. To allow the formation of a disulfide bond, the β-carbons of the two cysteines need to be in close proximity, *i.e.* 3–4 Å (21). We have now extended our studies to demonstrate that TMS3 of SecE forms an α-helix, with one face that stably interacts with TMS2 and TMS7 of SecY, whereas the opposite face dynamically interacts with TMS3 of a neighboring SecE molecule that is part of a separate SecYEG complex.

EXPERIMENTAL PROCEDURES

Materials—SecA (22), SecB (23), and proOmpA (24) were purified as described. A stock solution of 80 mM Cu^{2+}(phenantroline)$_3$ was prepared as described previously (19).

Plasmids—The plasmids used to overproduce SecYEG are listed in Table I. All mutations were introduced by a two-step polymerase chain

* This work was supported by the Council for Chemical Sciences of the Netherlands Organization for Scientific Research and subsidized by the Dutch Organization for the Advancement of Scientific Research. The costs of publication of this article were defrayed in part by the payment of page charges. This article must therefore be hereby marked "*advertisement*" in accordance with 18 U.S.C. Section 1734 solely to indicate this fact.

‡ To whom correspondence should be addressed. Tel.: 31-50-3632164; Fax: 31-50-3632154; E-mail: a.j.m.driessen@biol.rug.nl.

[1] The abbreviations used are: TMS, transmembrane segment; DTT, dithiothreitol; IMV, inner membrane vesicle; IPTG, isopropyl-1-thio-β-D-galactopyranoside; PAGE, polyacrylamide gel electrophoresis.

TABLE I
Plasmids

A synthetic *secYEG* operon behind the IPTG *trc* promotor was used for the plasmid-derived overexpression of the SecYEG complex. All listed plasmids were constructed via polymerase chain reaction mutagenesis, resulting in the indicated mutations. Double and triple cysteine mutants: the names are combined, e.g. pET2502/613 contains SecE V97C and SecY P276C mutations.

Plasmid	Relevant characteristic	Mutation	Source
pET324	p*trc*99A with LacZ in frame		Ref. 26
pET607	Cysteine-less SecYEG in pET610	C329S (TGT→AGT); C385S (TGC→AGC)	Ref. 19
	SecY TMS7 mutants in pET607		
pET611	V274C	V274C (GTA→TGT)[a]	Ref. 25
pET612	I275C	I275C (ATC→TGC)[a]	Ref. 25
pET613	P276C	P276C (CCG→TGT)[a]	Ref. 25
pET614	A277C	A277C (GCA→TGT)[a]	Ref. 25
pET615	I278C	I278C (ATC→TGC)[a]	Ref. 25
pET616	F279C	F279C (TTC→TGC)[a]	Ref. 25
pET617	A280C	A280C (GCT→TGT)[a]	Ref. 25
pET618	S281C	S281C (TCC→TGC)[a]	Ref. 25
pET2520	S282C	S282C (AGT→TGT)[a]	This work
	SecE TMS3 mutants in pET607		
pET627	L106C	L106C (CTG→TGT)[b]	Ref. 19
pET628	I107C	I107C (ATC→TGC)[b]	Ref. 19
pET2500	L95C	L95C (CTG→TGT)[b]	This work
pET2501	I96C	I96C (ATT→TGT)[b]	This work
pET2502	V97C	V97C (GTG→TGT)[b]	This work
pET2503	A98C	A98C (GCT→TGT)[b]	This work
pET2504	A99C	A99C (GCG→TGT)[b]	This work
pET2505	G110C	G110C (GGA→TGT)[b]	This work
pET2521	V100C	V100C (GTT→TGT)[b]	This work
pET2522	T101C	T101C (ACC→TGC)[b]	This work
pET2531	V97C/A99C	V97C (GTG→TGT); A99C (GCG→TGT)[b]	This work
pET2533	V97C/L106C	V97C (GTG→TGT); L106C (CTG→TGT)[b]	This work

[a] *secY* gene with *Bsp*EI (TCCGGT→TCCGGA).
[b] *secE* gene with Δ*Cla*I (ATCGAT→ATCGAC).

reaction using a template plasmid that allows overexpression of a cysteine-less SecYEG with an N-terminal His_6-tag on SecY (19). Cysteine mutagenesis was accompanied by the introduction of silent modifications in restriction sites to facilitate the screening for correct mutants. Single cysteine mutations in TMS7 of SecY were introduced together with a *Bsp*EI site in SecY (25). The introduction of single and double cysteine mutations in TMS3 of SecE was accompanied by the deletion of a *Cla*I site between SecY and SecE (19). All mutations were confirmed by complete sequence analysis.

Bacterial Strains, Growth Conditions, and Membrane Isolation—Cell growth and isolation of inner membrane vesicles (IMVs) was performed as described previously (19).

Cross-linking—For assays of disulfide bridge formation, IMVs (1 mg/ml) were incubated for 30 min at 37 °C in the presence of 1 mM $Cu^{2+}(phenantroline)_3$ (oxidized) or, as a control, with 5 mM dithiothreitol (DTT) (reduced). The oxidation reaction was quenched by the addition of 25 mM neocuproine (Sigma). Oxidized samples were "re-reduced" by the incubation in 100 mM of DTT for 1 h at 37 °C. Samples were analyzed by 12% SDS-PAGE and stained with Coomassie Brilliant Blue or further analyzed by Western blotting onto polyvinylidene difluoride membranes (Amersham Pharmacia Biotech) and immunostaining using antibodies against His-tagged SecY or SecE (26).

Miscellaneous Methods—Translocation reactions were performed as described before (19). Translocation ATPase of urea-treated IMVs was measured with proOmpA as substrate (27). Protein concentrations were determined by the method of Lowry *et al.* (28) in the presence of SDS using bovine serum albumin as a standard.

RESULTS

Construction, Expression, and Activity of Single-cysteine Mutants of SecE and SecY—Previously, we have described eight unique cysteine mutations that were introduced in TMS7 of SecY (Val-274 to Ser-281), covering at least two turns of the putative α-helical structure (25) (Table I). Sequence alignment and hydrophobicity analysis of the family of bacterial SecY proteins predicts the mutations in TMS7 of SecY to be located near the cytosolic membrane interface (Fig. 1). To investigate possible contacts between TMS3 of SecE and TMS7 of SecY, a new set of five unique cysteine mutations was made in TMS3 of SecE, covering positions Leu-95 to Ala-99 (Table I). These are predicted to be at the same membrane depth as the mutants in TMS7 of SecY (Fig. 1). The five cysteine mutations, together with mutation G110C in SecE, located close to the periplasmic membrane interface, were also used to further explore the contact interface with a neighboring TMS3 of SecE.

The single-cysteine SecE mutants were placed into a cysteine-less SecYEG expression vector (19) and overproduced in *E. coli* strain SF100. IMVs derived from these cells were analyzed for the SecY and SecE expression levels, SecA translocation ATPase activity, and proOmpA translocation. The expression levels of the various mutants as analyzed by SDS-PAGE and Coomassie Brilliant Blue staining were found to be identical to that of the overexpressed cysteine-less and wild-type SecYEG complex (data not shown). The proOmpA-stimulated SecA ATPase activity and the translocation of ^{125}I-labeled proOmpA of the mutants were indistinguishable from that of the cysteine-less and wild-type SecYEG complex (data not shown). None of the mutants was capable of translocating the proOmpA variant Δ8-proOmpA (data not shown), which carriers a defective signal sequence due to the deletion of Ile-8 (29). This substrate is effectively translocated by PrlA4 IMVs (30). Taken together, the data demonstrate that the introduction of the cysteines in respective positions of TMS3 of SecE does not alter the activity or specificity of the SecYEG complex.

SecE TMS3 Contacts a Neighboring SecE TMS3 at an α-Helical Interface—To investigate the contact interface between two TMS3 of SecE, IMVs containing overexpressed SecYEG complex harboring unique cysteine mutations in TMS3 of SecE (L95C, I96C, V97C, A98C, A99C, and G110C) were oxidized with $Cu^{2+}(phenantroline)_3$ and analyzed by SDS-PAGE and immunodetection using an antibody against SecE (Fig. 2*A*). Oxidation of the SecYE(A99C)G and SecYE(G110C)G com-

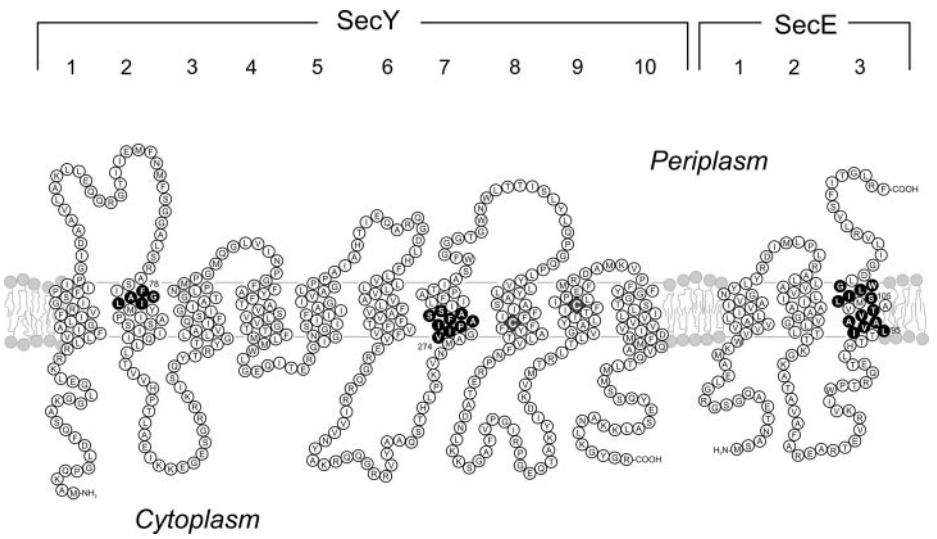

FIG. 1. **Membrane topology model of the *E. coli* SecY and SecE.** The *gray diamonds* represent the cysteine residues present in the wild-type SecY that were replaced by serine residues. The residues that were replaced by cysteine are indicated in *black circles*.

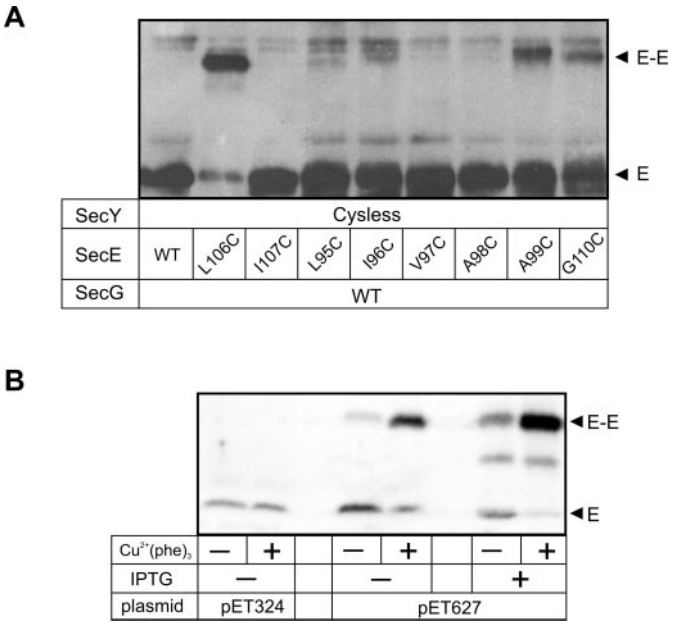

FIG. 2. **Mapping of the SecE-SecE contact interface.** *A,* IMVs containing overproduced amounts of SecYEG with the indicated single-cysteine mutation in TMS3 of SecE were oxidized with 1 mM Cu^{2+}(phenantroline)$_3$. Cysteine-less SecYEG and SecYE(I107C)G were included as a negative control, and SecYE(L106C)G was included as a positive control. *B,* IMVs were prepared from cells harboring pET324 (empty control plasmid) or pET627 (SecYE(L106C)G) grown in the presence of 0.5% glucose to suppress expression of the SecYEG complex. Samples were reduced (5 mM DTT) (–) or oxidized (1 mM Cu^{2+}(phenantroline)$_3$ ($Cu^{2+}(phe)_3$)) (+). As a control, a 25-fold diluted sample is shown that contained IMVs from cells induced for the overexpression of SecYE(L106C)G complex by IPTG. All samples were analyzed by 12% SDS-PAGE followed by immunoblotting using antibodies against SecE (*A*) or His-tagged SecE (*B*). The SecE monomer (*E*) and dimer (*E-E*) (28 kDa) are indicated by *arrowheads*.

plexes gave rise to a pronounced 28-kDa cross-linking product that is identical to the previously identified SecE-SecE cross-link found for the SecYE(L106C)G complex (19). The other single-cysteine SecE mutants did not yield a SecE-SecE cross-link. Modeling of the TMS3 of SecE as an α-helix structure shows that Ala-99, Leu-106, and Gly-110 are confined to the same face of the putative α-helix (Fig. 7). This result confirms the predicted α-helix structure of TMS3 of SecE and demonstrates that the interaction between neighboring SecE molecules is confined to a specific side of the α-helix.

To exclude the possibility that the formation of the SecE dimers was induced by the high concentration of SecYEG upon overexpression, the oxidation assay was repeated with IMVs containing low amounts of SecYE(L106C)G. A low level of SecYE(L106C)G production was achieved by growing cells harboring plasmid pET627 in the presence of 0.5% glucose and omitting IPTG to prevent induction of the *trc* promotor activity. Western blotting of dilution series showed no more than a 2–3-fold increase in the amount of SecE (see also Fig. 2*B*) and SecY (data not shown) as compared with the endogenous level. Overexpression upon induction by IPTG resulted in at least 250-fold increase in the SecYEG level (data not shown, and see Fig. 2*B*). Samples of IMVs derived from cells harboring pET324 (empty control vector) and pET627 (SecYE(L106)G) with or without induction of overexpression by IPTG were analyzed after oxidation by SDS-PAGE and immunodetection using an antibody against His-tagged SecE (Fig. 2*B*). Oxidation of IMVs harboring low amounts of SecYE(L106C)G resulted in the efficient cross-linking of the SecE dimer (Fig. 2*B*). This demonstrates that the formation of this complex also occurs at levels of SecYEG that are comparable to those found in wild-type membranes.

SecE TMS3 Contacts SecY TMS7—To identify further contacts between SecE and SecY, the single-cysteine mutations in SecE TMS3 (L95C, I96C, V97C, A98C, A99C) and SecY TMS7 (V274C, I275C, P276C, A277C, I278C, F279C, A280C, and S281C) were co-expressed yielding 40 pairs of cysteine mutants. The activity of the SecY TMS7 mutants have been analyzed previously, and all mutants behave normally except for SecY(I278C)EG that exhibits a *prlA* phenotype (25). All pairs of cysteine mutants showed normal levels of overexpression (Fig. 3*A*; data not shown). IMVs were oxidized with Cu^{2+}(phenantroline)$_3$ and analyzed by SDS-PAGE and Coomassie Brilliant Blue staining (Fig. 3*A*) or immunoblotting using antibodies against SecY and SecE (Fig. 3*B*; data not shown). For two double-cysteine combinations, a higher molecular mass band was observed upon oxidation at the position of an expected SecY-SecE cross-link. The formation of the cross-link product of SecY(P276C) and SecE(V97C) was very efficient, resulting in a nearly complete disappearance of monomeric SecY and SecE. This result implies a stoichiometric interaction between SecE and SecY that was previously assumed but not demonstrated experimentally. Cross-linking between SecY(P276C) and E(L95C) was less efficient. Modeling shows that both contacts cannot be confined to the same α-helical face between the corresponding transmembrane segments (Fig. 7*A*).

SecY TMS7 and SecE TMS3 Contact Interface Is α-Heli-

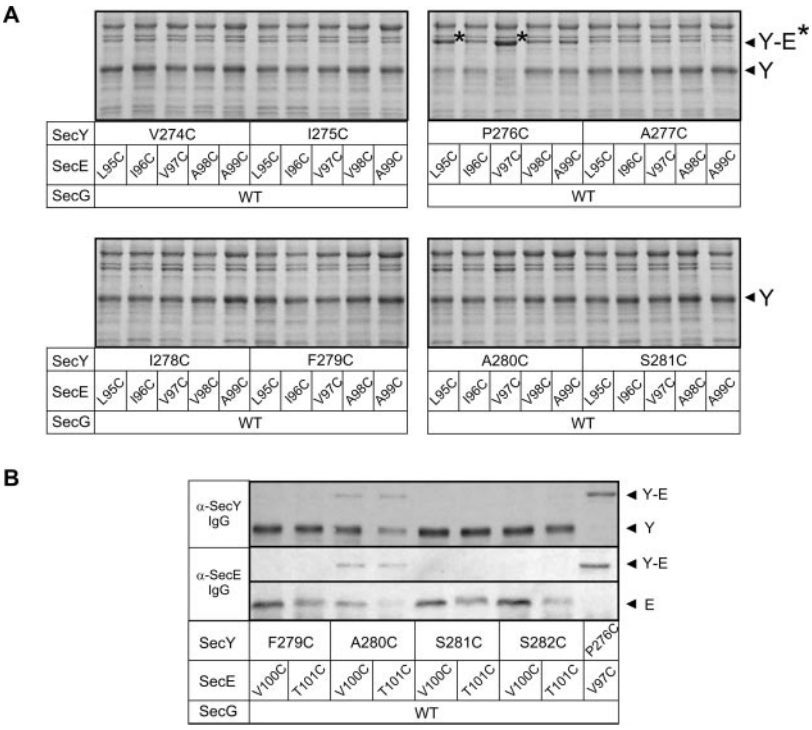

FIG. 3. **Mapping of the contact interface between TMS7 of SecY and TMS3 of SecE.** *A,* eight consecutive unique cysteine mutations in TMS7 of SecY (V274C, I275C, P276C, A277C, I278C, F279C, A280C, and S281C) were co-expressed with five cysteine mutations in TMS3 of SecE (L95C, I96C, V97C, A98C, and A99C) and SecG. IMVs containing the mutant SecYEG complexes were oxidized with 1 mM Cu^{2+}(phenantroline)$_3$ and analyzed by 12% SDS-PAGE and Coomassie Brilliant Blue staining. The disulfide cross-linked SecY-SecE complexes (50 kDa) are indicated on the gel by an *asterisk*. *WT,* wild-type. *B,* four consecutive unique cysteine mutations in TMS7 of SecY (F279C, A280C, S281C, and S282C) were co-expressed with two cysteine mutations in TMS3 of SecE (V100C and T101C) and SecG. Cross-links were identified as described above, and analyzed by SDS-PAGE and immunoblotting using antibodies against His-tagged SecY and SecE. The cross-link between SecY(P276C) and SecE(V97C) was included as a control. SecY (*Y*) and SecY-SecE cross-link (*Y-E*) (50 kDa) are indicated by *arrowheads*.

cal—To further investigate the structure of the interface between SecY TMS7 and SecE TMS3, additional double-cysteine combinations were constructed of residues that are located deeper in the membrane. Four SecY TMS7 cysteine mutations (F279C, A280C, S281C, and S282C) were combined with two additional SecE TMS3 cysteine mutations (V100C and T101C). The respective SecYEG complexes again exhibit normal overexpression levels and translocation activities (data not shown). Upon the oxidation of the pairs of cysteine mutants, two additional SecY-SecE cross-links could be identified after SDS-PAGE and immunoblotting using antibodies against SecY and SecE (Fig. 3*B*). These cross-links occurred between SecY(A280C) and SecE(V100C) or SecE(T101C), but the efficiency was less as compared with the SecY(P276C)-SecE(V97C) combination. Modeling of TMS7 of SecY and TMS3 of SecE as α-helical segments shows that these newly identified contacts are confined to the same helical interface as the SecY(P276C)-SecE(V97C) cross-link (Fig. 7). Because the cross-link between SecY(P276C) and SecE(L95C) cannot be modeled into this α-helical interface, we assume that SecE Leu-95 is located outside the membranous environment in a non-α-helical structure (Fig. 7*B*).

Interaction between SecY and SecE within an Oligomeric SecYEG Complex—Because the SecY(P276C)-SecE(V97C) and intermolecular SecE(L106C) cross-links are very strong, a triple-cysteine mutant of the SecYEG complex was constructed to determine whether such contacts occur within an oligomeric SecYEG complex. IMVs prepared from cells expressing the SecY(P276C)E(V97C/L106C)G showed normal levels of overproduction (data not shown) and activity (Fig. 5). Immunodetection of oxidized samples showed the presence of strong SecY-(SecE)$_2$ and weaker (SecY)$_2$-(SecE)$_2$ cross-link products (Fig. 4). Similar but less efficient cross-link products could be demonstrated for a SecY(P276C)E(V97C/A99C)G mutant (data not shown). These data therefore suggest that the identified SecE-SecE cross-links are at a contact interface between two separate SecYEG complexes. In all samples, a band was observed that stains with the antibody against SecE at the position of SecY-(SecE)$_2$ (Fig. 4). However, this band is unrelated to these proteins, as it was also present in the reduced samples and it did not stain with the antibody against SecY. Furthermore, in all samples, a diffuse protein band was detected that stains with the SecY antibody and that migrates with a molecular mass that is between that of the SecY-(SecE)$_2$ and (SecY)$_2$-(SecE)$_2$ cross-linking products (Fig. 4). Because this band was observed also with the cysteine-less SecYEG complex, albeit weaker, we assume that it represents an aggregated SecY dimer, the formation of which is stimulated by the oxidation.

SecY-SecE and SecE-SecE Cross-linking Reversibly Inactivate the Translocase—IMVs harboring overexpressed cysteine-less SecYEG, SecYE(L106C)G, SecY(P276C)E(V97C)G, and SecY(P276C)E(V97C/L106C)G were assayed for the effect of cross-linking on the translocation activity. IMVs were either reduced in the presence of DTT or oxidized with Cu^{2+}(phenantroline)$_3$. Oxidized samples were re-reduced by the incubation in DTT, and the activity was assayed by the translocation of ^{125}I-proOmpA (Fig. 5). The activity of the cysteine-less SecYEG was not affected by the oxidation-reduction conditions. Under oxidizing conditions, however, translocation of proOmpA proceeded only to the I_{29} intermediate due to the presence of a disulfide bond in the C-terminal end of proOmpA (19). All three cysteine mutant SecYEG complexes displayed normal activity under reduced condition but were nearly completely inactive under oxidizing conditions. With all mutants, substantial activity could be recovered after re-reduction of the samples.

The Interhelical SecY TMS7-SecE TMS3 Contact Is Retained during Translocation—Using the thiol-mediated contact between neighboring SecE molecules as a molecular ruler, we have shown previously that during the initiation of preprotein translocation, the intermolecular SecE contact is enhanced (19). To investigate the dynamics of the SecY-SecE contact, the same technique was employed using the SecY(P276C)E(V97C)G complex. IMVs were preincubated in DTT, incubated under various translocation conditions, and subsequently oxidized with Cu^{2+}(phenantroline)$_3$ to probe for the efficiency of SecY-SecE cross-linking. Because formation of the SecY-SecE contact is already very efficient under nontranslocating conditions, a less-than-optimal condition of oxidation (on ice) was applied to be able to detect changes in the cross-

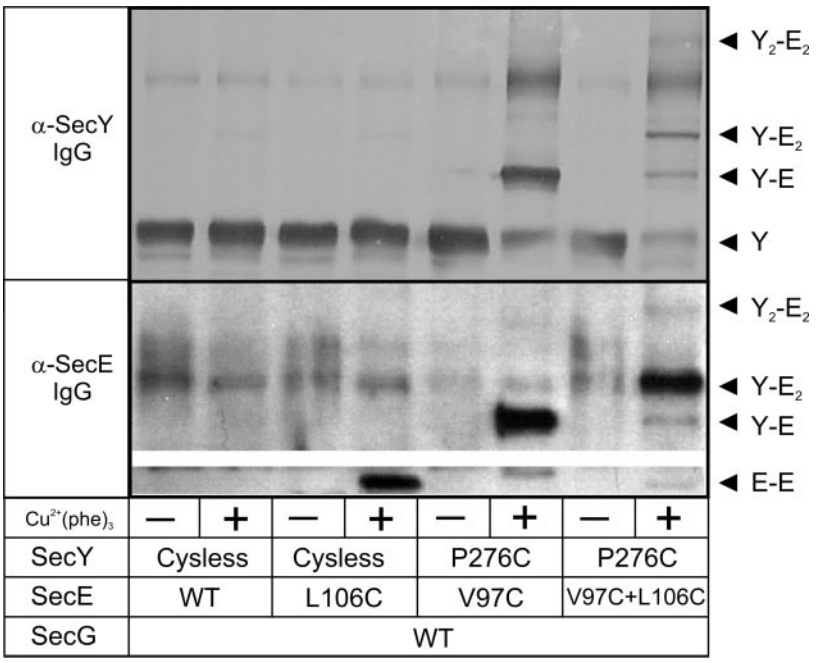

FIG. 4. **Disulfide cross-linking of a SecYE dimer.** IMVs containing the cysteine-less SecYEG, SecYE(L106C)G, SecY(P276C)E(V97C)G, and SecY(P276C-)E(V97C/L106C)G were reduced with 5 mM DTT (–) or oxidized with 1 mM Cu^{2+}(phenantroline)$_3$ ($Cu^{2+}(phe)_3$) (+). Samples were analyzed by 12% SDS-PAGE and immunostaining using antibodies against His-tagged SecY and SecE. The SecE-SecE (*E-E*), SecY-SecE (*Y-E*), SecY-(SecE)$_2$ (*Y-E$_2$*), and (SecY)$_2$-(SecE)$_2$ (*Y$_2$-E$_2$*) cross-links are indicated with *arrowheads*.

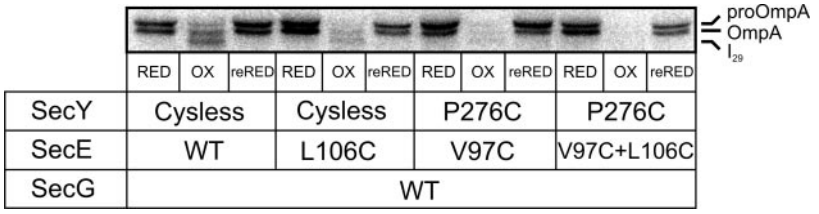

FIG. 5. **Disulfide cross-linking of the SecYEG complex reversibly inactivates proOmpA translocation.** IMVs containing the cysteine-less SecYEG, SecYE(L106C)G, SecY(P276C)E(V97C)G and SecY(P276C)E(V97C/L106C)G were reduced with 5 mM DTT (*RED*) or oxidized with 1 mM Cu^{2+}(phenantroline)$_3$ (*OX*). A sample of the oxidized samples was re-reduced by incubation in 100 mM DTT (*reRED*). IMVs were supplemented with SecA and assayed for the translocation of ^{125}I-proOmpA as described under "Experimental Procedures." The positions of proOmpA, OmpA, and the translocation intermediate I_{29} are indicated.

linking efficiency. Translocation conditions were induced by the addition of SecA and the preprotein proOmpA in the presence of ATP, AMP-PNP, or ATP in the presence of the SecA ATPase inhibitor azide (31). None of these conditions, however, resulted in a significant change in the efficiency of the SecY-SecE cross-linking (Fig. 6). Therefore, it is concluded that TMS7 of SecY and TMS3 of SecE remain in close proximity during protein translocation.

DISCUSSION

Cysteine scanning mutagenesis is a technique that can be used to map the sites of contacts between the helices in membrane proteins. We have used this technique to obtain more detailed information about the interaction of the two essential components SecY and SecE of the protein-conducting channel of *E. coli*. This study provides experimental evidence that TMS3 of SecE forms an α-helix with one face contacting a neighboring SecE molecule, whereas the other face contacts TMS7 (this study) and TMS2 (19) of SecY.

Previously, we have identified position Leu-106 of TMS3 of SecE as a site of contact with a neighboring SecE molecule (19). In that study, five unique cysteine substitutions were introduced near the periplasmic membrane interface of TMS3 of SecE (S105C–W109C) in order to cover a complete turn of an α-helix. To determine whether this contact interface extends along the entire putative α-helical structure, six additional cysteine mutants were made close to the cytosolic (L95C–A99C) and periplasmic (G110C) membrane interface. In this screen, we now have identified two additional amino acid residues in TMS3 of SecE that map at the interface between two SecE molecules, *i.e.* Ala-99 and Gly-110. Modeling of TMS3 of SecE as an α-helical structure demonstrates that these residues are strictly confined to a specific side of the α-helix (Fig. 7). Interestingly, the cross-linking efficiency for the L106C mutation is significantly higher than for A99C and G110C. This could mean that the two contacting transmembrane segments are tilted or twisted relative to each other, with an optimal point of contact around Leu-106.

By combining a set of single cysteine mutants in TMS7 of SecY (V274C–S282C) (25) with mutants in TMS3 of SecE (L95C–T101C), several sites of contact between SecY and SecE could be detected. In particular, SecY(P276C) to SecE(V97C) could be efficiently cross-linked (Figs. 3 and 4). The same position of SecY also cross-linked to SecE(L95C), albeit with low efficiency (Fig. 3*A*). SecY(A280C) was found to contact both SecE(V100C) and SecE(T101C) (Fig. 4). The identified sites of contact fit with an α-helical contact interface, except for the SecY(P276C)-SecE(L95C) interaction (Fig. 7). Considering the low efficiency of cross-linking of the latter cysteine pair, and the uncertainty in predicting the borders of the TMSs, it seems likely that Leu-95 of SecE is located outside the membrane plane and is not part of the α-helical structure of TMS 3. This is illustrated in Fig. 7*B*.

The cross-linking of SecY(P276C) with SecE(V97C) was nearly complete, leaving little nonreacted monomeric SecY and SecE upon oxidation. This implies that there is only one SecE molecule per SecY subunit in the SecYEG complex. In this respect, their interdependent stability (12, 13), similar levels of overexpression (32), and well defined regions of interaction (14,

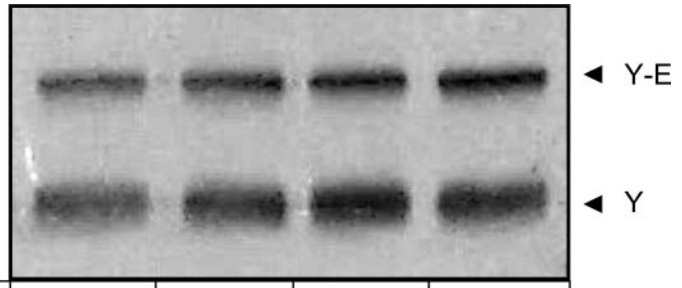

SecA	—	+	+	+
ATP	—	+	—	+
AMP-PNP	—	—	+	—
NaN_3	—	—	—	+
proOmpA	+	+	+	+

FIG. 6. **The interaction between TMS7 of SecY and TMS3 of SecE is not modulated during preprotein translocation.** IMVs containing the SecY(P276C)E(V97C)G complex were prereduced with 5 mM DTT and diluted into translocation mixtures (50 μl) containing 50 mM HEPES-KOH, pH 7.5, 30 mM KCl, 5 mM $Mg(Ac)_2$. The reaction mixture was supplemented with 1 μg of proOmpA, 1 μg of SecA, 2 mM ATP or AMP-PNP, and 20 mM sodium azide (NaN_3) as indicated. After 10 min of incubation at 37 °C, 1 mM Cu^{2+}(phenantroline)$_3$ was added, and the incubation was continued on ice for 30 min. Oxidation was terminated by the addition of 25 mM neocuproine, and the samples were analyzed by 12% SDS-PAGE and immunostaining using antibodies against His-tagged SecY or SecE (data not shown). The positions of SecY and the SecY-SecE cross-link are indicated with *arrowheads*.

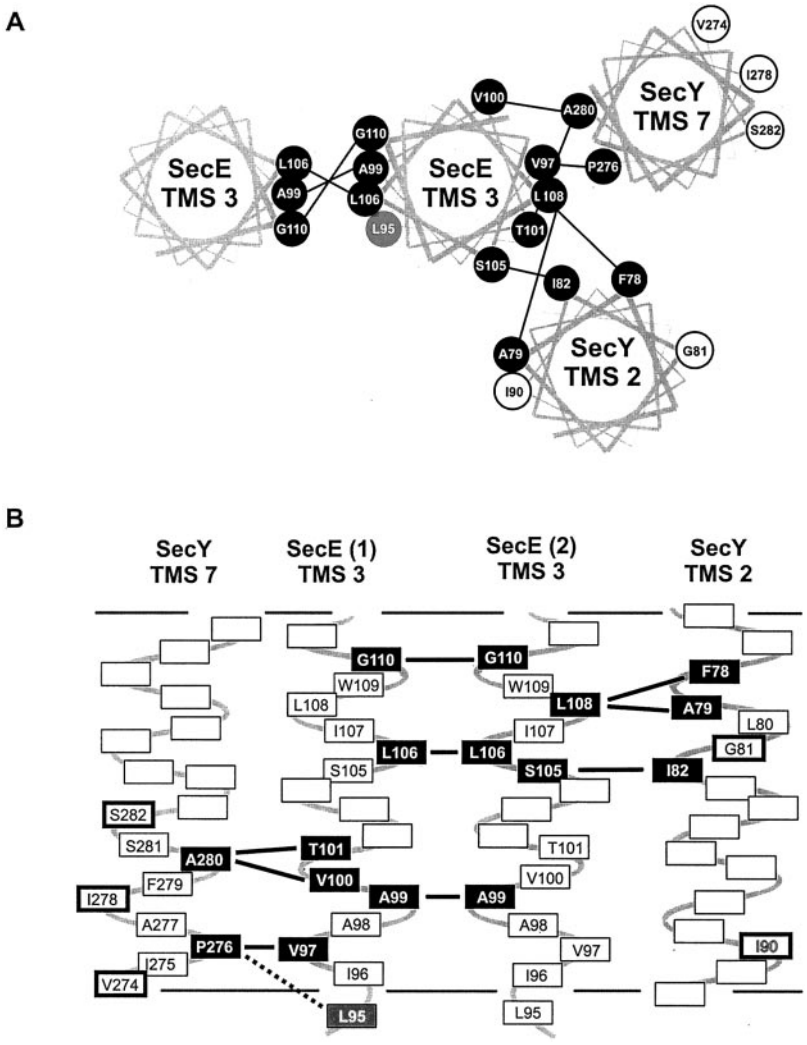

FIG. 7. **Schematic representation showing the identified sites of interaction between TMS2 and TMS7 of SecY and TMS3 of SecE, and the identified sites of interaction between TMS3 of neighboring SecE molecules.** *A, top view*. TMSs are schematically drawn as helices. Cysteine-substituted residues involved in the cross-linking are shown (*closed circles*) and connected by a *line* to the interacting amino acid residues. Sites of *prlA* mutations are depicted as *open circles*. *B, side view*. Interacting cysteine-substituted residues are indicated in *black boxes,* and sites of known *prlA* mutations are depicted in *thicker outlined boxes*. The sites of interaction are shown by *connecting lines*. The weak cross-link between Leu-95 of SecE and Pro-276 of SecY is indicated by a *dotted line*.

17–19) are consistent with the experimentally determined SecY-SecE stoichiometry.

The cysteine scanning mutagenesis (Ref. 19 and this study) now provides a detailed image of the molecular environment of SecE TMS3 (Fig. 7). Herein, TMS3 of SecE is surrounded by another TMS3 of SecE and TMS2 and TMS7 of SecY. In the current arrangement, there is ample space for at least one other SecE contacting helix. Based on the predictions made

using the synthetic lethality of combinations of *prlA* and *prlG* mutants (17), TMS 10 of SecY seems a likely candidate. It is of interest to note that the amino acid residue positions that cause the synthetic lethality of *prlA208* (SecY TMS7, I278N) with *prlG1* (SecE TMS3, L108R) do not map at the SecY TMS7-SecE TMS3 contact interface (Fig. 7). The same holds true for all of the *prlA* mutations that map in TMS2 and TMS7 of SecY. None of these amino acid residues face TMS3 of SecE, but instead they point in the opposite direction (Fig. 7). Strikingly, these mutations lead to a destabilization of the SecY-SecE interaction (33), in particular when PrlA and PrlG mutants are combined (17).

Biochemical and electron microscopic studies (8, 34) suggest that the SecYEG complex oligomerizes to form a protein conducting channel. The structure consists of a tetrameric SecYEG complex with an outer diameter of 10.5–12 nm and a central pore-like opening (8). The shape of the tetrameric SecYEG complex resembles that of the ribosome-bound purified eukaryotic Sec61p complex visualized by cryo-electron microscopy, which is a ring-like structure 5–6 nm high and ~9 nm wide (35, 36). The cylindrical pore of ~2 nm in diameter extends throughout the protein complex perpendicular to the plane of the membrane, and aligns with the protein exit tunnel of the ribosome (35). A recent chemical cross-linking and immunoprecipitation study failed to demonstrate an oligomeric SecYEG complex, and it was suggested that the SecYEG complex functions as a monomer (37). It was argued that the formation of an oligomeric SecYEG complex is an artifact of high overproduction levels and purified proteins. Our specific cysteine-mutagenesis assay demonstrates that the oligomeric SecYEG complex can also be formed at SecYEG levels comparable to that of wild-type. Yahr and Wickner (37) used the nonspecific cross-linker formaldehyde in their study. SecY is, however, very unstable in the presence of low concentrations of organic solvents, such as ethanol and formaldehyde, and it readily denatures. This may explain the failure to detect SecY-SecY and SecY-SecA cross-links (38). Interestingly, a recent paper on the projection structure of the SecYEG complex indicates that the molecule is arranged as a dimer in the crystal lattice (39). Moreover, the same study shows by analytical ultracentrifugation, a monomer-dimer-tetramer equilibrium of the SecYEG complex. Also, by blue native PAGE, the presence of oligomeric SecYEG complexes is evident.[2] Taken together, these studies strongly suggest that the SecYEG complex is able to assemble into oligomeric structures.

We have combined the strong SecY(P276C)-SecE(V97C) and SecE(L106C)-SecE(L106C) contacts by means of a triple-cysteine mutant. Oxidation of the SecY(P276C)SecE(V97C/L106C)G complex clearly demonstrates the formation of products that correspond to SecY-$(SecE)_2$ and $(SecY)_2$-$(SecE)_2$ cross-links. This unequivocally demonstrates that the SecE-SecE interaction takes place at a contact interface between two neighboring SecYEG complexes. Another cysteine scanning mutagenesis study demonstrates that two SecG molecules are in close proximity (40). It should be stressed that disulfide cross-linking is a very sensitive technique that detects sites of interaction only when they are in close proximity, *i.e.* within a distance of 3–4 Å (21). Taken together, these data collaborate with the electron microscopy studies that demonstrate that the SecYEG complex can oligomerize into a large complex (8).

The formation of thiol-stabilized SecY-SecE and SecE-SecE contacts reversibly inactivates the activity of the translocase (Fig. 5) (19). Apparently, flexibility within and between SecYEG complexes is an essential requirement for the translocation mechanism. This may signify conformational changes or dynamic subunit interactions during the translocation reaction, as previously shown for the SecE-SecE contact (19). By blocking SecA membrane de-insertion, a significant enhancement of the SecE-SecE cross-linking efficiency was observed. This phenomenon strictly required the presence of a preprotein showing its relation to the translocation process. On the other hand, the same conditions do not result in an alteration of the SecY-SecE cross-linking as shown for the interaction between SecE TMS3 with SecY TMS2 (19) and SecY TMS7 (Fig. 6). A cross-linking study with the yeast Sec61α, a SecY homolog, demonstrates the signal sequence of an inserting preprotein contacts TMS7 and TMS2, whereas no contact could be detected with Sec61γ (20). This has led to the hypothesis that Sec61γ (*i.e.* TMS3 of SecE) might function as a kind of mock signal sequence that is displaced from Sec61α (*i.e.* SecY) upon the insertion of the signal sequence of a preprotein (20). This mechanism is not plausible for the SecYEG complex as the interaction between TMS2 and TMS7 of SecY with TMS3 of SecE stably persists during translocation. It seems more likely that the signal sequence contacts the helical faces of TMS2 and TMS7 that point away from TMS3 of SecE. Remarkably, these faces correspond to the sites of the PrlA mutations (Fig. 7).

The hypothesis that SecYEG functions as monomer (37) requires a large rearrangement of the SecYEG helices in order to open a translocation pore that can accommodate the inserting SecA molecule and preprotein (41) while shielding SecA from contact with the phospholipids phase (42, 43). Our studies do not support such large helical rearrangements, as both TMS2 and TMS7 of SecY remain in close proximity to TMS3 of SecE during translocation. Rather, our studies indicate the recruitment of multiple SecYEG complexes much akin to a "rigid body" assembly event. To further test this model, future biochemical experiments should be directed at the mapping of the intramolecular contacts between the helices within the SecY protein.

Acknowledgments—We thank Jeanine de Keyzer, Jelto Swaving, Nico Nouwen, Andreas Kaufmann, and Erik Manting for fruitful discussions and technical assistance.

REFERENCES

1. Driessen, A. J. M., Manting, E. H., and van der Does, C. (2001) *Nat. Struct. Biol.* **8,** 492–498
2. Schiebel, E., Driessen, A. J. M., Hartl, F. U., and Wickner, W. T. (1991) *Cell* **64,** 927–939
3. Economou, A., and Wickner, W. T. (1994) *Cell* **78,** 835–843
4. van der Wolk, J. P., de Wit, J. G., and Driessen, A. J. M. (1997) *EMBO J.* **16,** 7297–7304
5. Brundage, L., Hendrick, J. P., Schiebel, E., Driessen, A. J. M., and Wickner, W. T. (1990) *Cell* **62,** 649–657
6. Hanada, M., Nishiyama, K. I., Mizushima, S., and Tokuda, H. (1994) *J. Biol. Chem.* **269,** 23625–23631
7. Hartl, F. U., Lecker, S., Schiebel, E., Hendrick, J. P., and Wickner, W. T. (1990) *Cell* **63,** 269–279
8. Manting, E. H., van der Does, C., Remigy, H., Engel, A., and Driessen, A. J. M. (2000) *EMBO J.* **19,** 852–861
9. Pohlschroder, M., Prinz, W. A., Hartmann, E., and Beckwith, J. (1997) *Cell* **91,** 563–566
10. Gorlich, D., Prehn, S., Hartmann, E., Kalies, K.-U., and Rapoport, T. A. (1992) *Cell* **71,** 489–503
11. Schatz, P. J., Bieker, K. L., Ottemann, K. M., Silhavy, T. J., and Beckwith, J. (1991) *EMBO J.* **10,** 1749–1757
12. Joly, J. C., Leonard, M. R., and Wickner, W. T. (1994) *Proc. Natl. Acad. Sci. U. S. A.* **91,** 4703–4707
13. Kihara, A., Akiyama, Y., and Ito, K. (1995) *Proc. Natl. Acad. Sci. U. S. A.* **92,** 4532–4536
14. Baba, T., Taura, T., Shimoike, T., Akiyama, Y., Yoshihisa, T., and Ito, K. (1994) *Proc. Natl. Acad. Sci. U. S. A.* **91,** 4539–4543
15. Pohlschroder, M., Murphy, C., and Beckwith, J. (1996) *J. Biol. Chem.* **271,** 19908–19914
16. Osborne, R. S., and Silhavy, T. J. (1993) *EMBO J.* **12,** 3391–3398
17. Flower, A. M., Osborne, R. S., and Silhavy, T. J. (1995) *EMBO J.* **14,** 884–893
18. Harris, C. R., and Silhavy, T. J. (1999) *J. Bacteriol.* **181,** 3438–3444
19. Kaufmann, A., Manting, E. H., Veenendaal, A. K. J., Driessen, A. J. M., and van der Does, C. (1999) *Biochemistry* **38,** 9115–9125
20. Plath, K., Mothes, W., Wilkinson, B. M., Stirling, C. J., and Rapoport, T. A. (1998) *Cell* **94,** 795–807

[2] de Keyzer, J., unpublished results.

21. Hazes, B., and Dijkstra, B. W. (1988) *Protein Eng.* **2,** 119–125
22. Cabelli, R. J., Chen, L., Tai, P. C., and Oliver, D. B. (1988) *Cell* **55,** 683–692
23. Weiss, J. B., Ray, P. H., and Bassford, P. J., Jr. (1988) *Proc. Natl. Acad. Sci. U. S. A.* **85,** 8978–8982
24. Crooke, E., Guthrie, B., Lecker, S., Lill, R., and Wickner, W. T. (1988) *Cell* **54,** 1003–1011
25. Manting, E. H., Kaufmann, A., van der Does, C., and Driessen, A. J. M. (1999) *J. Biol. Chem.* **274,** 23868–23874
26. van der Does, C., Manting, E. H., Kaufmann, A., Lutz, M., and Driessen, A. J. M. (1998) *Biochemistry* **37,** 201–210
27. Lill, R., Cunningham, K., Brundage, L. A., Ito, K., Oliver, D., and Wickner, W. T. (1989) *EMBO J.* **8,** 961–966
28. Lowry, O. H., Rosebrough, N. J., Farr, A. L., and Randall, R. J. (1951) *J. Biol. Chem.* **193,** 265–275
29. Tanji, Y., Gennity, J., Pollitt, S., and Inouye, M. (1991) *J. Bacteriol.* **173,** 1997–2005
30. van der Wolk, J. P., Fekkes, P., Boorsma, A., Huie, J. L., Silhavy, T. J., and Driessen, A. J. M. (1998) *EMBO J.* **17,** 3631–3639
31. Oliver, D. B., Cabelli, R. J., Dolan, K. M., and Jarosik, G. P. (1990) *Proc. Natl. Acad. Sci. U. S. A.* **87,** 8227–8231
32. Matsuyama, S., Akimaru, J., and Mizushima, S. (1990) *FEBS Lett.* **269,** 96–100
33. Duong, F., and Wickner, W. T. (1999) *EMBO J.* **18,** 3263–3270
34. Meyer, T. H., Ménétret, J. F., Breitling, R., Miller, K. R., Akey, C. W., and Rapoport, T. A. (1999) *J. Mol. Biol.* **285,** 1789–1800
35. Beckmann, R., Bubeck, D., Grassucci, R., Penczek, P., Verschoor, A., Blobel, G., and Frank, J. (1997) *Science* **278,** 2123–2126
36. Ménétret, J., Neuhof, A., Morgan, D. G., Plath, K., Radermacher, M., Rapoport, T. A., and Akey, C. W. (2000) *Mol. Cell* **6,** 1219–1232
37. Yahr, T. L., and Wickner, W. T. (2000) *EMBO J.* **19,** 4393–4401
38. Manting, E. H., van der Does, C., and Driessen, A. *J. M. (1997) J. Bacteriol.* **179,** 5699–5704
39. Collinson, I., Breyton, C., Duong, F., Tziatzios, C., Schubert, D., Or, E., Rapoport, T., and Kuhlbrandt, W. (2001) *EMBO J.* **20,** 2462–2471
40. Nagamori, S., Nishiyama, K., and Tokuda, H. (2000) *J. Biochem. (Tokyo)* **128,** 129–137
41. Eichler, J., and Wickner, W. T. (1997) *Proc. Natl. Acad. Sci. U. S. A.* **94,** 5574–5581
42. Eichler, J., Brunner, J., and Wickner, W. T. (1997) *EMBO J.* **16,** 2188–2196
43. van Voorst, F., van der Does, C., Brunner, J., Driessen, A. J. M., and de Kruijff, B. (1998) *Biochemistry* **37,** 12261–12268